EUROPEAN JOURNAL OF PHARMACEUTICAL SCIENCES 33 (2008) 42–51

available at www.sciencedirect.com

ScienceDirect

journal homepage: www.elsevier.com/locate/ejps

PLA-PEG nanocapsules radiolabeled with ^{99m}Technetium-HMPAO: Release properties and physicochemical characterization by atomic force microscopy and photon correlation spectroscopy

Maira Alves Pereira[a], *Vanessa Carla Furtado Mosqueira*[b,*], *José Mário Carneiro Vilela*[c], *Margareth Spangler Andrade*[c], *Gilson Andrade Ramaldes*[d], *Valbert Nascimento Cardoso*[a]

[a] *Departamento de Análises Clínicas, Faculdade de Farmácia, Universidade Federal de Minas Gerais, Av. Antônio Carlos 6627, Belo Horizonte, MG 31270-901, Brazil*

[b] *Departamento de Farmácia, Escola de Farmácia, Universidade Federal de Ouro Preto, Rua Costa Sena, 171 Centro, Ouro Preto, MG 35400-000, Brazil*

[c] *Fundação Centro Tecnológico de Minas Gerais (CETEC), Avenida José Cândido da Silveira 2000, Belo Horizonte, MG 31170-000, Brazil*

[d] *Departamento de Produtos Farmacêuticos, Faculdade de Farmácia, Universidade Federal de Minas Gerais, Av. Antônio Carlos 6627, Belo Horizonte, MG 31270-901, Brazil*

ARTICLE INFO

Article history:
Received 4 November 2006
Received in revised form
15 August 2007
Accepted 18 September 2007
Published on line 29 September 2007

Keywords:
Nanocapsules
Atomic force microscopy
^{99m}Technetium-HMPAO
Physicochemical characterization
Photon correlation spectroscopy
Radiotracer

ABSTRACT

The present work describes the preparation, characterization and labelling of conventional and surface-modified nanocapsules (NC) with ^{99m}Tc-HMPAO. The size, size distribution and homogeneity were determined by photon correlation spectroscopy (PCS) and zeta potential by laser doppler anemometry. The morphology and the structural organization were evaluated by atomic force microscopy (AFM). The stability and release profile of the NC were determined in vitro in plasma. The results showed that the use of methylene blue induces significant increase in the encapsulation efficiency of ^{99m}Tc-HMPAO, from 24.4 to 49.8% in PLA NC and 22.37 to 52.93% in the case of PLA-PEG NC ($P < 0.05$) by improving the complex stabilization. The average diameter of NC calculated by PCS varied from 216 to 323 nm, while the average diameter determined by AFM varied from 238 to 426 nm. The AFM analysis of diameter/height ratios suggested a greater homogeneity of the surface-modified PLA-PEG nanocapsules compared to PLA NC concerning their flattening properties. The in vitro release of the ^{99m}Tc-HMPAO in plasma medium was faster for the conventional PLA NC than for the surface-modified NC. For the latter, 60% of the radioactivity remained associated with NC, even after 12 h of incubation. The results suggest that the surface-modified ^{99m}Tc-HMPAO-PLA-PEG NC was more stable against label leakage in the presence of proteins and could present better performance as radiotracer in vivo.

* *Corresponding author*. Tel.: +55 31 35591638; fax: +55 31 35591628.
E-mail address: mosqueira@ef.ufop.br (V.C.F. Mosqueira).

0928-0987/$ – see front matter © 2007 Elsevier B.V. All rights reserved.
doi:10.1016/j.ejps.2007.09.007

1. Introduction

Over the last few decades, several radiopharmaceuticals have been developed for the detection of infection and inflammation (Oyen et al., 1996a; Chianelli et al., 1997; Rennen et al., 2001). There is an ongoing search for new and better radiopharmaceuticals having high sensitivity and specificity (Laverman et al., 1999). Accurate and rapid detection of infection and inflammatory lesions facilitate both the elucidation of the course of the disease and the installation of a tailored therapeutic regimen. One approach involves the use of radiolabeled nanocarriers to target infection and inflammation improving their scintigraphic acquisitions, because they could be able to permeate to the interstitial space passing through the leaky capillaries of the inflammatory regions, by passive targeting. Long-circulating (Stealth™) nanocarriers can theoretically allow radiotracer delivery to sites outside MPS (Oyen et al., 1996b).

Nanocapsules (NC) are submicronic nanoparticulate carriers composed of an oily core surrounded by a polymeric wall with lipophilic and/or hydrophilic surfactants at the interface (Legrand et al., 1999). The ability of NC to improve the biopharmaceutical properties of lipophilic substances has been demonstrated (Barratt, 2000; Mosqueira et al., 2006; Sasatsu et al., 2006) and has generated great interest for use as diagnostic agents. However, conventional nanoparticles are rapidly cleared from the circulation by phagocytes of the mononuclear phagocyte system (MPS) (Gref et al., 1994). Surface modification of nanocapsules with hydrophilic polymers, such as polyethyleneglycol (PEG), resulted in decreased recognition by the MPS, thereby increasing the half-life of their circulation in the blood stream (Mosqueira et al., 1999, 2001b).

Technetium-99m D,L-hexamethylpropyleneamine oxime (^{99m}Tc-HMPAO) is a radiopharmaceutical widely used to obtain scintigraphic images, especially for cerebral diagnosis. ^{99m}Tc-HMPAO is especially used for blood cells labelling to obtain images of infections and inflammations because of its lipophilic properties (Martin-Comin and Prats, 1999). As shown in Fig. 1, radiolabeling of D,L-HMPAO may give rise to two ^{99m}Tc-labelled enantiomers with almost identical properties (Vanderghinste et al., 2003). The employment of the ^{99m}Tc-HMPAO complex in the preparation of new types of radiopharmaceuticals such as the radiolabeled liposomes has been studied by several authors (Goins et al., 1993; Phillips, 1998; Laverman et al., 1999; Boerman et al., 2000). However, studies with liposomes have been limited because of inherent problems such as low encapsulation efficiency, poor storage stability (Soppimath et al., 2001) and a high incidence of side effects after i.v. administration (Brouwers et al., 2000; Dams et al., 2000; Szebeni et al., 2000, 2002).

The NC presents high entrapment efficiency for lipophilic drugs, a low polymer content and a low inherent toxicity when compared with liposomes and nanospheres (Mosqueira et al., 2006). Nevertheless, before utilizing a NC formulation for diagnosis, it must be very well characterized. Optimal preparations consist of a small (200–300 nm), monodispersed nanocapsule population, stable in biological media, principally in blood. Ruozi et al. (2005) obtained information about the dimensions and homogeneity of liposomes using classical photon correlation spectroscopy (PCS) and atomic force microscopy (AFM). Recently, the AFM method was also used to characterize nanocapsules prepared with biodegradable polymers (Mosqueira et al., 2005; Leite et al., 2005; Assis et al., 2007).

The aim of the present work was the preparation and characterization of the conventional and the sterically stabilized NC using poly-D,L-lactide (PLA) polymer and the copolymer of monomethoxypolyethyleneglycol-co-poly-D,L-lactide (PLA-PEG), respectively, for the encapsulation of ^{99m}Tc-HMPAO complex. Furthermore, it was also investigated the labelling efficiency of NC with ^{99m}Tc-HMPAO complex and its release profiles in physiological media.

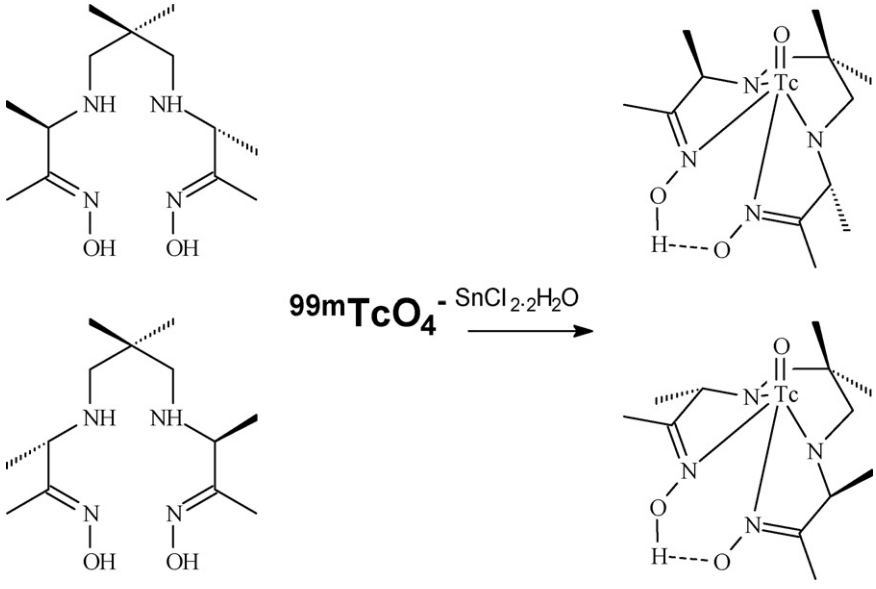

Fig. 1 – The chemical structures of D,L isomers of HMPAO and their reaction with ^{99m}Technetium to form lipophilic complex. Redrawn and adapted from Vanderghinste et al. (2003).

2. Materials and methods

2.1. Materials

Soy lecithin (Epikuron® 170) was purchased from Lucas Meyer (France). Poly(D,L-lactic acid), $PLA_{50,}$ with an average molecular weight (Mw) of 75,000(g/mol) and the surfactant poloxamer 188 were provided by Sigma–Aldrich (USA). Miglyol 810N (caprylic/capric triglycerides) was received as a gift from Hulls (Germany). PLA-PEG (PLA of 49,000 g/mol containing approximately 10% PEG covalently grafted with a Mw of 5000 g/mol) was provided by Alkermes (USA) and used without further purification. The HMPAO (D,L-hexamethylpropyleneamine oxime) was obtained by reconstitution of a Ceretec kit (Amersham Inc., UK) and ^{99m}Tc (pertechnetate form) was obtained as a sodium solution from a ^{99}Mo generator (IPEN/Brazil). All the solvents used were analytical grade, and other chemicals were commercially available reagent grade and used without further purification. MilliQ® water (Simplicity 185, Millipore, Bedford, USA) was used throughout.

2.2. Methods

2.2.1. Preparation of nanocapsules

Conventional nanocapsules (PLA NC) were prepared according to the method described by Fessi et al. (1989) and those sterically stabilized with PEG were prepared by the method described by Mosqueira et al. (2001a). In the conventional NC preparation poly(D,L-lactic acid) (Mw 75,000) was used together with Poloxamer 188, a surfactant containing polyethyleneglycol chains on its chemical structure. Surface-modified NC was prepared using the diblock polymer of PLA-PEG without poloxamer surfactant. In the PLA-PEG NC the PEG chains are covalently linked to NC surface. Briefly, the polymer (0.6%, w/v) was dissolved in acetone (2 mL) containing 0.75% (w/v) of soy lecithin (Epikuron® 170) and 2.5% (v/v) of Miglyol® 810N. In the case of conventional NC, this organic solution was poured into the external aqueous phase (4 mL) containing 0.75% (w/v) of poloxamer 188 with stirring. The solvents were evaporated under reduced pressure up to 2 mL volume (Fisatom Rotary Evaporator, Brazil).

2.2.2. ^{99m}Tc-HMPAO-labelled nanocapsules preparation

An HMPAO kit (Ceretec®, Amersham Inc., UK) containing 0.5 mg HMPAO and 4.0 μg $SnCl_2$ was reconstituted with 2 mL of 0.9% NaCl solution. The mixture was divided into four aliquots of 0.4 mL each and stored at −70 °C under a nitrogen atmosphere. Aliquots (0.4 mL) of HMPAO were incubated with 296 MBq of $Na^{99m}TcO_4$ for 5 min and 250 μL of methylene blue solution was added. Methylene blue was used to stabilize the lipophilic ^{99m}Tc-HMPAO complex (Barthel et al., 1999). The radiolabeled complex was then dissolved in the organic phase (acetone) during the preparation of the nanocapsules. The following steps of the procedure were carried out as described above to obtain the ^{99m}Tc-HMPAO nanostructures.

2.2.3. Purification of ^{99m}Tc-HMPAO-NC

^{99m}Tc-HMPAO that was not associated with NC was separated from the ^{99m}Tc-HMPAO loaded in NC by gel filtration through a Sephadex G-25 (Pharmacia®, Sweden) column. A 1 mL aliquot of a colloidal suspension of ^{99m}Tc-HMPAO-NC was layered onto a 1.5 cm × 15 cm Sephadex G-25 column, and the sample was eluted with saline. One-millilitre fractions were collected and counted in a scintillation counter (Capintec, INC-CRC.15R, USA). An aliquot (1 mL) containing unloaded NC and free ^{99m}Tc-HMPAO was passed through the column to determine the difference in the separation profiles of the preparations. The small amounts of ^{99m}Tc-HMPAO complex used in this work were soluble in water (manufacturer, Ceretec-Amersham Health). The purified ^{99m}Tc-HMPAO-NC was used in further characterization experiments.

2.2.4. ^{99m}Tc-HMPAO encapsulation efficiency and release

The encapsulation efficiency of ^{99m}Tc-HMPAO in the nanocapsules was calculated by the difference between the total activity of the lipophilic complex in the colloidal suspension and the free ^{99m}Tc-HMPAO found in the external aqueous phase (Eq. (1)). The ultrafiltrate (external aqueous phase) was obtained by ultrafiltration/centrifugation of 400 μL of NC suspension at 1800 × *g* for 15 min in an AMICON device (Microcon, Millipore®, molecular weight cut-off: 10,000). The ^{99m}Tc-HMPAO released from NC formulations was determined in 70% rat plasma under sink conditions at different times. Aliquots containing 3.7 MBq of ^{99m}Tc-HMPAO-PLA-PEG NC and ^{99m}Tc-HMPAO-PLA NC (200 μL) were incubated with 500 mL of plasma (70%) at 37 °C, under moderate stirring, in separated tubes for each time point. After 30, 120, 480 and 720 min samples (200 μL) were collected to radioactivity determination in a gamma counter, after external phase separation from the total NC suspension, using the ultrafiltration/centrifugation technique with Ultrafree® units, 0.1 μm pore size (Millipore®). The separation membrane used in the release study allowed the elution of the free ^{99m}Tc-HMPAO complex or that was associated with plasmatic protein, while the ^{99m}Tc-HMPAO entrapped in NC remained in the membrane upper compartment. An additional experiment was performed in plasma medium with ^{99m}Tc-HMPAO encapsulated in PLA-PEG NC during NC preparation or ^{99m}Tc-HMPAO incubated with unloaded PLA-PEG NC. This analysis was evaluated in time periods of up to 720 min. These experiments were also performed at 37 °C with moderate stirring. The non-encapsulated ^{99m}Tc-HMPAO was encountered in the ultrafiltrate, and the encapsulated ^{99m}Tc-HMPAO was retained by the ultrafiltration membrane. The encapsulation efficiency of radioactivity into the NC was determined from following Eq. (1), where *A* = activity:

$$(\%) = \frac{A^{\text{total}} - A^{\text{ultrafiltrate}}}{A^{\text{total}}} \times 100 \quad (1)$$

2.2.5. Nanocapsules characterization

2.2.5.1. *Photon correlation spectroscopy analysis*. The mean size and size distribution of the NC was determined by photon correlation spectroscopy. This method allows the determination of the mean diameter of the particle and the polydispersity index (PI), which is a dimensionless measure of the broadness of the particle size distribution. Particle size was evaluated in a Zetasizer HS3000 (Malvern Instruments, Malvern, UK). Samples were analyzed after appropriate dilution in ultra-pure MilliQ water. Reported values were

expressed as mean ± standard deviation for at least three different batches of each nanocapsule formulation.

2.2.5.2. *Atomic force microscopy imaging*. AFM observation was performed in air at room temperature, on a Dimension 3000 apparatus, as well as on Multimode Equipment, both monitored by a Nanoscope IIIa controller from Digital Instruments (Santa Barbara, CA, USA). A droplet (5 μL) of sample was deposited on a freshly cleaved mica surface, spread and partially dried with a stream of argon. The images were obtained in tapping mode, using commercial silicon probes, from Nanosensors™, with cantilevers having a length of 228 μm, resonance frequencies of 75–98 kHz, spring constants of 29–61 N/m and a nominal tip curvature radius of 5–10 nm. The scan rate used was 1 Hz. Dimensional analyses were performed using the "section of analyses" program of the system. A minimum of ten images from each sample was analyzed to assure reproducible results. The values represent an average ± standard deviation of approximately 40 particle measurements.

2.2.5.3. *Zeta potential analyses*. The zeta potential was determined by laser doppler anemometry (LDA) in a Zetasizer HS3000 (Malvern Instruments, Malvern, UK). The samples were analyzed following dilution by 1:1000 in 1 mM NaCl at a conductivity of approximately 120 ± 20 μS/cm^2. Values reported are the mean ± standard deviation of at least three different batches of each NC formulation.

2.2.6. *Statistics*

All experiments were performed in triplicate and were expressed as mean values ± standard deviations, except as otherwise stated. Mean sizes, zeta potential and drug release data at each time point were compared by an ANOVA test using the Prim 4.0 program while considering a probability of 5% to be significant.

3. Results and discussion

NC containing ^{99m}Tc-HMPAO were prepared by the interfacial deposition of the preformed polymer followed by solvent evaporation (Fessi et al., 1989), a simple and rapid method of obtaining nanocapsules containing a radioactive tracer suitable for intravenous administration. All formulations described here produced particles smaller than 500 nm and greater than 200 nm. Normal tissues contain capillaries with tight junctions that are less permeable to nanosized particles (Litzinger et al., 1994). The different types of NC produced in this work are intended to be used as radiotracers of inflammation sites where the capillaries are very leaky. In this way, the sizes found were considered suitable for the further purpose. Two types of nanocapsules containing ^{99m}Tc-HMPAO were developed in this work: conventional PLA NC and surface-modified PLA-PEG NC. Surface-modified nanocapsules (PLA-PEG NC) were included in this study because their uptake by the mononuclear phagocyte system is substantially delayed, thereby increasing the time during which they circulate in the blood stream (Mosqueira et al., 2001b).

Table 1 – Effect of methylene blue on the encapsulation efficiency of ^{99m}Tc-HMPAO complex in polymeric NC

Formulation	^{99m}Tc-HMPAO encapsulation efficiency (% A_{NC}/A_T)[a]	
	Without MB	With MB
PLA NC	24.40 ± 0.79 a	49.80 ± 1.35 b
PLA-PEG NC	22.37 ± 1.50 a	52.93 ± 2.91 b

Identical letters indicate that there is no significant difference between the data. The data represent the mean ± S.D. (n = 3) for each determination.

[a] A_{NC} is activity associated to the NC and A_T is the total activity in NC suspension (Bq).

3.1. *Nanocapsule characterization*

A better encapsulation efficiency of the ^{99m}Tc-HMPAO complex in the nanocapsules was obtained using methylene blue as a stabilizer. According to the results shown in Table 1, the encapsulation efficiency was around 50% for both preparations (PLA NC and PLA-PEG NC). On the other hand, the encapsulation efficiency of ^{99m}Tc-HMPAO in NC preparations without methylene blue was greatly reduced. Thus, the stability of the lipophilic ^{99m}Tc-HMPAO complex was enhanced by methylene blue, as has been reported in a previous work (Barthel et al., 1999; Sobal and Sinzinger, 2001).

The particle size, polydispersity index and zeta potential of prepared conventional and surface-modified NC containing ^{99m}Tc-HMPAO are presented in Table 2. The polydispersity indices showed that the different formulations prepared by the nanoprecipitation method were homogeneous with respect to the polydispersity index and can be considered monodisperse (≤0.3). The PLA-PEG NC showed reduced sizes compared to the PLA NC by the both methods used to determine NC mean sizes (Table 2). These results are in agreement with the data obtained by Mosqueira et al. (2001a) for PLA and PLA-PEG NC, however, the NC sizes were slightly different from those previously reported, probably because the average molecular weights of the polymers were different and obtained from other suppliers. The mean diameters of unloaded and ^{99m}Tc-HMPAO loaded NC were very similar and no significant difference were found among the preparations. ^{99m}Tc-HMPAO encapsulation in PLA and PLA-PEG NC did not induce any significant increase in the mean diameter and in the polydispersity of the colloidal NC suspensions. Some authors have demonstrated that the mean diameter of nanoparticles has an influence on the biodistribution studies because particles larger than 300 nm and lower than 70 nm are rapidly taken up by MPS accumulating in the spleen and liver. On the other hand, particles within the 150–200 nm range were founded to be longest circulating (Litzinger et al., 1994; Owens and Peppas, 2006). Based on this observation, the long-circulating PLA-PEG NC, with sizes around 200 nm, could be particularly interesting to reach the loose junctions of the endothelium of inflammatory or infectious foci, considering the mean sizes measured by PCS. In fact, biodistribution studies performed in our laboratory (data not published) showed that ^{99m}Tc-HMPAO-PLA-PEG NC were able to identify inflammatory foci up to 12 h after administration when injected

Table 2 – Physicochemical characteristics of the NC preparations

NC formulation	Mean size ± S.D.[a] (nm) (PCS)	Mean size ± S.D.[a] (nm) (AFM)	Polydispersity index[b]	ζ potential ± S.D.[a] (mV)[c]
PLA	282 ± 24	411 ± 128	0.335	−61.8 ± 4.4
^{99m}Tc-HMPAO-PLA	323 ± 37	426 ± 105	0.266	−62.0 ± 1.7
PLA-PEG	216 ± 36	238 ± 124	0.229	−57.9 ± 1.8
^{99m}Tc-HMPAO-PLA-PEG	267 ± 27	387 ± 104	0.300	−60.3 ± 1.5

The entrapment of ^{99m}Tc-HMPAO did not significantly affect either the mean diameter or the zeta potential of the nanocapsules ($P > 0.05$).
[a] Standard deviation ($n = 3$) of the population that was reported by the instrument.
[b] Monodispersed samples (≤0.3).
[c] Measurement after 1:1000 dilution in 1 mM NaCl (conductivity, 120 ± 20 μS/cm).

intravenously in rats. Both types of PEG chains associated with a NC surface, adsorbed (Poloxamer 188) or covalently grafted (PLA-PEG copolymer), seemed to stabilize the association of ^{99m}Tc-HMPAO with the nanostructures, thereby preventing their aggregation, because no signs of physical instability were observed during the experiments even when PLA or PLA-PEG NC were incubated in 70% rat plasma release media.

Zeta potential results (Table 2) showed that the unloaded PLA NC and ^{99m}Tc-HMPAO loaded NC formulations exhibited a negative charge with values ranging from −57.9 to −62.0 mV. The entrapment of ^{99m}Tc-HMPAO did not significantly affect either the mean diameter or the zeta potential of the nanocapsules ($P > 0.05$) indicating that probably the complex was mainly associated with the oily core of NC. These values were typically observed for colloidal carriers containing PLA polymer, where values of −50.9 to −51 mV were found for PLA-POLOX NC and PLA-PEG NC 45–5 kDa (10% PEG), respectively, prepared from polymers with slightly different Mw and using the same method (Mosqueira et al., 2001a, 2006). The negative zeta potential imparted by the PLA polymer and lecithin was not masked by the presence of PEG chains with its hiding properties, probably because the high contents of lecithin in the NC formulation contributed to the maintenance of the negative surface charge, as has been previously discussed by Mosqueira et al. (2001a, 2006). However, even when these negatively charged PLA-PEG NC were used in vivo (Mosqueira et al., 2001b) they showed long-circulating properties, probably because lecithin layers surrounding NC masks the real zeta potential at NC interfaces. In general, nanospheres, without lecithin and oil, suffer a much higher effect of PEG on the zeta potential than NC (Govender et al., 2000).

AFM is a powerful technique, with dimensional resolutions from 1 up to 100 Å, that provides a unique possibility for visualizing nanoparticles in a natural environment, without sample manipulation (Neves et al., 1998). While PCS measures hydrodynamic radius, the AFM technique allows direct measurement of size in samples in a partially dried state, deposited on freshly cleaved mica plates, which permits simultaneous characterization of particle shape and structure. It is advantageous because the size, structure and shape are important parameters in the design of nanostructures used in diagnosis by an intravenous route. All NC preparations showed a spherical form on the mica surface in the AFM images (Figs. 2 and 3). The NC maintained their structures unaltered for up to 1 week after drying. The NC presented a homogeneous distribution in height and in three-dimensional images (Fig. 3). The average sizes of unloaded PLA NC obtained by AFM were 411 ± 128 nm, while those containing ^{99m}Tc-HMPAO were 426 ± 105 nm ($n = 40$). Similarly, when the NC size was determined by PCS, no significant differences were observed between unloaded NC and those containing the ^{99m}Tc-HMPAO complex. However, the diameters calculated by AFM were observed to be larger than those measured by PCS for both NC types. This observation can be explained by a possible NC flattening on mica that takes place after drying process with argon flow. The PLA NC images (Fig. 4) show nanostructures and layers deposited on the mica with different heights, resulting in complex images when compared with PLA-PEG. These few nanometer layers (2–10 nm) were attributed to poloxamer and phospholipids organized in lamellar structures, as could be observed in the analysis images obtained from these controls (poloxamer and lecithin). Similar observations were previously reported by Leite et al. (2005). NC in all samples appears deposited on these layers or immersed in them (Fig. 4). On the other hand, PLA-PEG NC (Fig. 2C and D) presents more homogeneous distribution of particles with the absence of the low height layered structures. It could be explained by the absence of poloxamer in the PLA-PEG formulation that reduces the complexity of forms in the system. The average diameter calculated for PLA-PEG NC was 238 ± 124 nm ($n = 40$) and for ^{99m}Tc-HMPAO-PLA-PEG NC was 387 ± 104 nm ($n = 40$). The mean size differences were not significant ($P > 0.05$). In fact, the flattening process was probably related to variations in polymeric wall thickness and homogeneity of polymer deposition in the process of NC preparation, as previously speculated by Leite et al. (2005). The greater the thickness of the polymeric wall, the greater its hardness and the lower the NC ability to flatten in mica plates would be. This result implies that NC wall variations, such as the PEG chemical grafting could produce different degrees of flattening. The ratios between diameter/height were calculated from the topographical profile from AFM images (Fig. 5). A certain percentage of these heterogeneities were observed in NC polymeric wall formation for all the preparations. The PLA NC wall heterogeneities were greater because the diameter/height ratios varied from 1 to 10, indicating no uniform deposition of the polymer on the surface. This hypothesis is also supported by the use of cross-linking agent to increase polymeric wall hardness of PLA and PLA-PEG NC before AFM analysis, which reduces dramatically the diameter/height ratios (Assis et al., 2007). Furthermore, the formation of other nanostructures, such

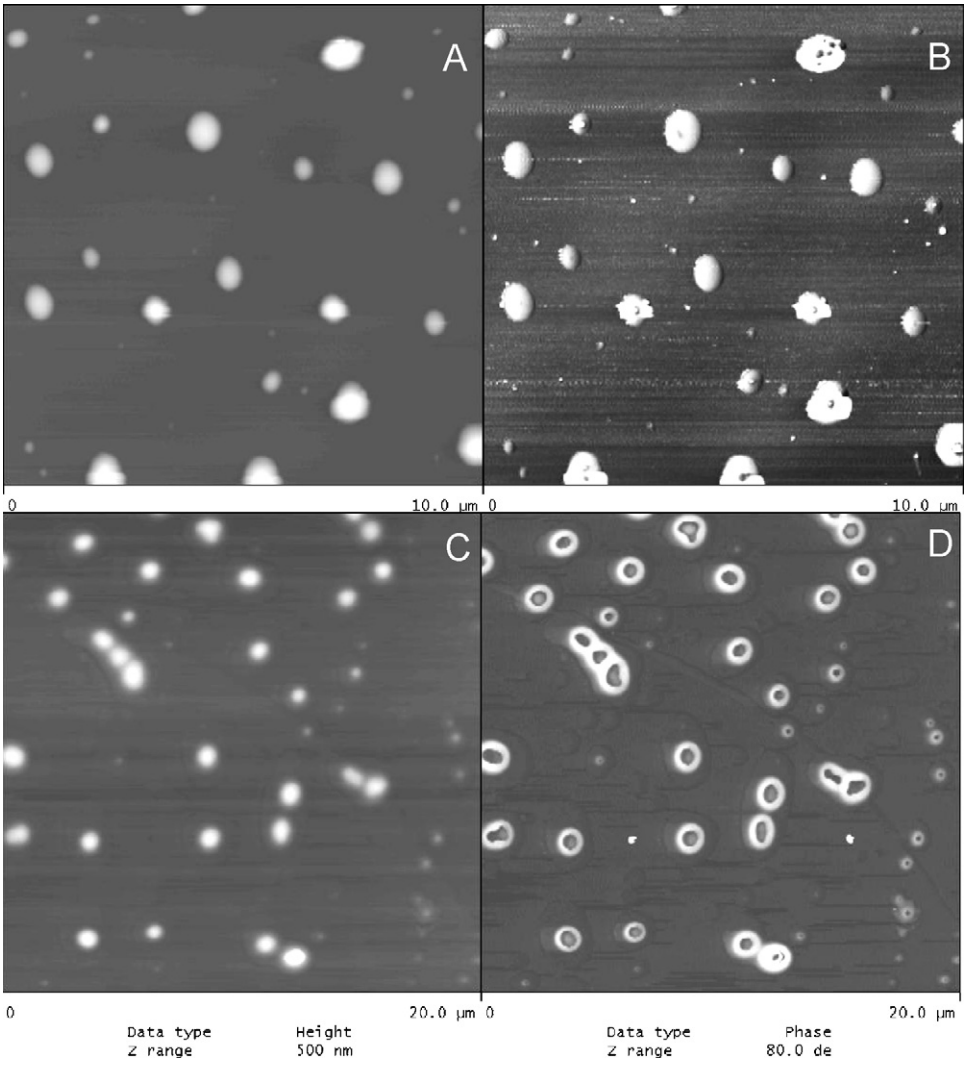

Fig. 2 – AFM topographic (height) images A (PLA NC) and C (PLA-PEG NC) and phase images B (PLA NC) and D (PLA-PEG NC) showing spherical nanocapsules obtained in tapping mode. Scan sizes are shown in the figure.

as nanospheres, or even nanoemulsions (without polymeric wall) could occur. This result agrees with those observed by Mosqueira et al. (2001a), which demonstrated the complexity of the nanostructures formed by the nanoprecipitation method and the increase in homogeneity of PLA-PEG NC prepared without poloxamer using ultracentrifugation in Percoll® gradient method. The PLA-PEG NC presented a more homogeneous wall with diameter/height ratios of 4–7 (Fig. 5C and D). ^{99m}Tc-HMPAO associated with PLA-PEG NC increased the NC dispersion heterogeneity and diameter/height difference (7–10), probably because it produced alterations in the structure of NC wall. Poloxamer seemed also to play a role in the formation of different types of nanostructures in NC formulations and in the appearance of complex layers in AFM images that probably increase the heterogeneity of PLA NC (Fig. 4). The evidence of NC wall formation and the determination of its thickness was elegantly performed by Rübe et al. (2005) using the small angle neutron scattering technique applied to NC prepared by the same nanoprecipitation method used in this paper.

In PLA-PEG NC images obtained by AFM, a halo was observed around the NC (Fig. 2D). The phase images suggest that this phenomenon could be generated by a hydration layer around sterically stabilized PLA-PEG NC, probably because a small amount of water are firmly fixed to the hydrophilic groups by hydrogen bonds at NC surface and was not completely removed by the fast argon flow that spread the sample on mica. It is noteworthy to point out that this halo was not observed by AFM in PLA NC stabilized with poloxamer and appears particularly in the phase images of PLA-PEG NC (Fig. 2D). This structure in halo form suggests the presence of covalently grafted PEG in this preparation.

Comparing PCS with AFM, the second technique allows one to perceive differences in NC structures related to the polymeric wall that produce different degrees of flattening in mica plates. This behaviour identified by AFM technique proved that NC has a fluid core and a heterogeneous wall thickness, while PCS technique furnished a homogeneous distribution of nanoparticles with any information about their structural properties and shape.

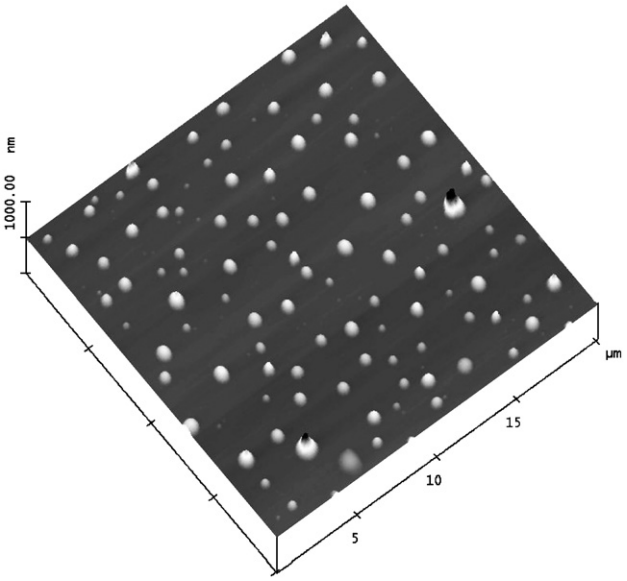

Fig. 3 – AFM image: three-dimensional view of unloaded PLA nanocapsules spread on mica and its homogenous dispersion of size.

3.2. ^{99m}Tc-HMPAO release from nanocapsules

The in vitro release profiles of ^{99m}Tc-HMPAO from PLA and PLA-PEG nanocapsules are shown in Fig. 6. The experiments were preformed under sink conditions to avoid the interference of the complex solubility in the release rate. In this study a fast release of radioactivity for all NC types was observed in the first 30 min. Approximately 33% of ^{99m}Tc-HMPAO was released in plasma medium for PLA-PEG NC. This result can be explained by the release of an adsorbed part of the ^{99m}Tc-HMPAO weakly bound to the NC surface, or by a fast equilibrium changes in the partition between internal oily core and release medium. Plasma probably acts as a driving force that promotes ^{99m}Tc-HMPAO release from the NC in the burst phase. In the case of NC, a fast release of drug in the first few minutes after dilution in release media was interpreted by several authors as drug adsorbed at the NC surface (Lopes et al., 2000; Mosqueira et al., 2001b, 2006). However, the release profile of ^{99m}Tc-HMPAO was biphasic, because after the initial burst phase (30 min) only 7% of the radioactivity was released from NC up to 12 h (Fig. 6). Phillips (1998) has shown that liposomes are able to retain ^{99m}Tc-HMPAO in plasma at 37 °C for as much as 90 h. However, comparative and quantitative analysis of the ability of the both nanosystems to entrap this radiotracer have not been performed and should be evaluated in further experiments. On the other hand, when the ^{99m}Tc-HMPAO was only incubated with the already formed PLA-PEG

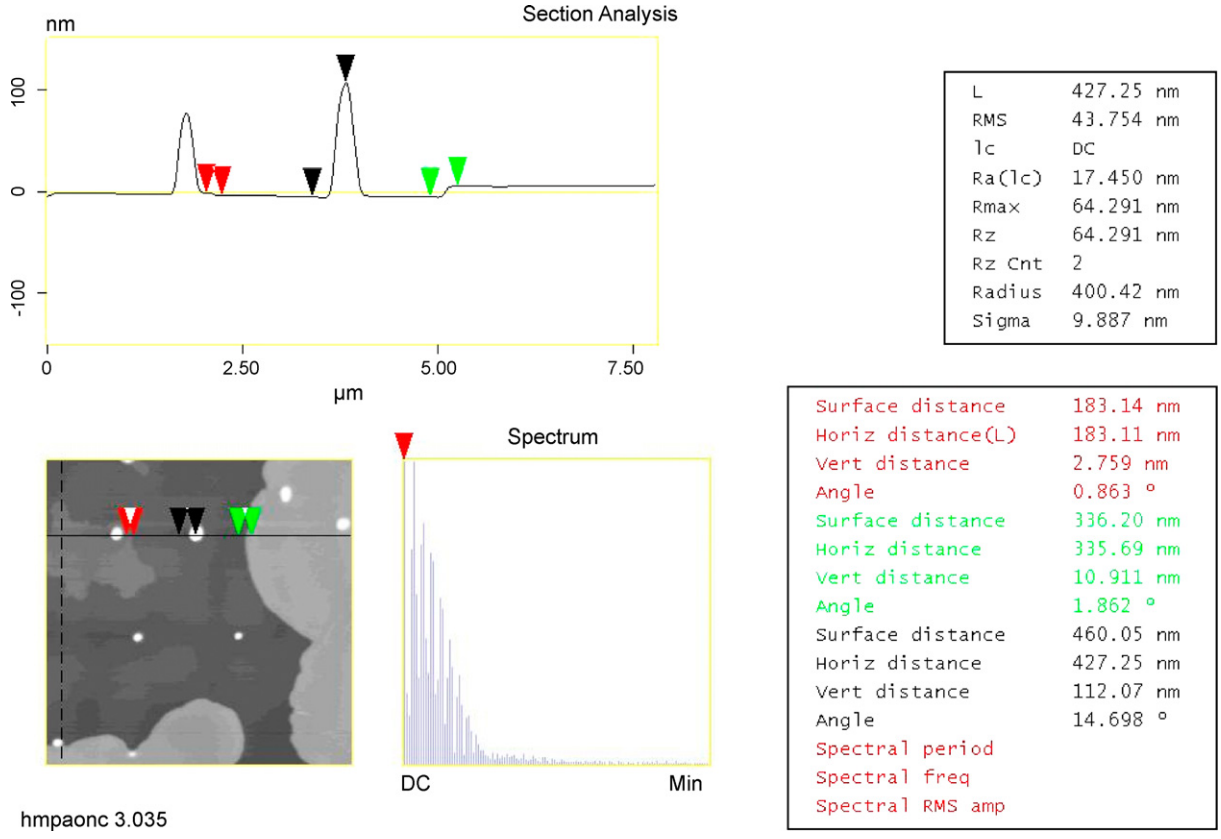

Fig. 4 – AFM image of ^{99m}Tc-HMPAO-PLA nanocapsules in the "section analysis" software showing nanocapsule height in black arrows, and different nanometric layers deposed on mica indicated by red and green arrows (height). The measured sizes are indicated in tables with the same colours. Scan size: 7.5 μm × 7.5 μm. (For interpretation of the references to color in this figure legend, the reader is referred to the web version of the article.)

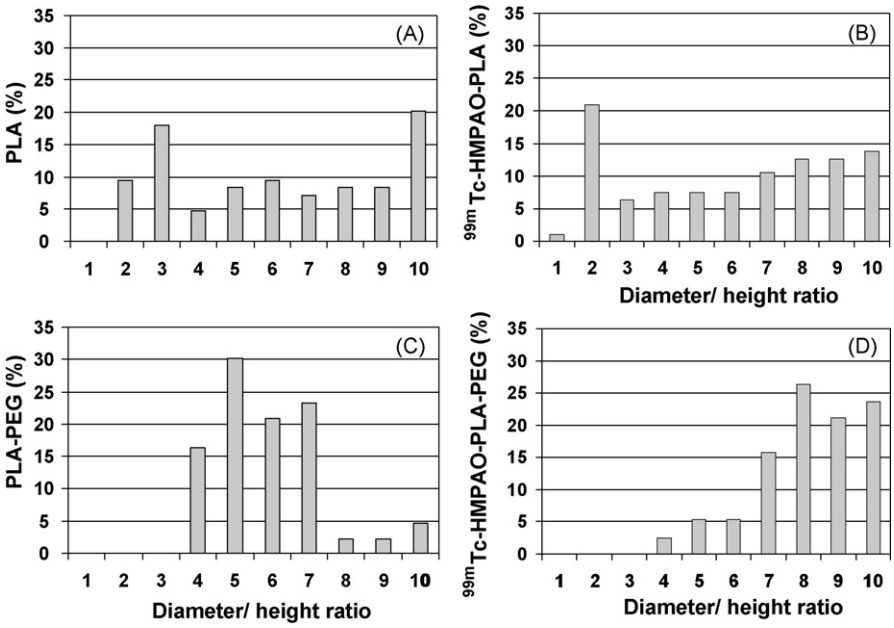

Fig. 5 – Percentage of diameter/height ratios of nanocapsules preparations calculated from 40 particles measurements using "section analysis software" of the Nanoscope IIIa AFM microscope. In A: unloaded PLA NC; B: ^{99m}Tc-HMPAO-PLA NC; C: unloaded PLA-PEG NC; D: ^{99m}Tc-HMPAO-PLA-PEG NC. The higher ratios indicate higher degrees of nanocapsule flattening on mica surface.

NC, 70% of the radioactivity was released in the first 30 min and 90% in 120 min, suggesting that in this case ^{99m}Tc-HMPAO was not truly encapsulated into the NC structure, being rapidly desorbed when in contact with the release media. Lopes et al. (2000), in a similar experiment, observed a total release of the ethionamide after incubation with preparations of nanocapsules and nanospheres. Based on these results, they proposed that the drug might be mainly bound to the particle's surface. After the initial burst, ^{99m}Tc-HMPAO that seems to be firmly associated to PLA-PEG NC structure, release less than 10% of the total radioactivity in the first 12 h in medium with 70% of plasma. This result indicates that PLA-PEG NC is more able to retain ^{99m}Tc-HMPAO compared to PLA NC. Cruz et al. (2006) also evidenced a biphasic release profile from NC, attributing the burst phase to the presence of the polymer, whereas the presence of the oil increased the half-life of the sustained phase. The release profiles of ^{99m}Tc-HMPAO from the NC, despite of the type of the polymer, are in agreement with those cited above, however the rates could not be compared because the release media was different. In this way, a relationship between PLA-PEG polymer and the radioactive complex could explain the reduced initial burst, although this is not completely understood. Furthermore, the halo visualized in AFM images surrounding PLA-PEG NC could represent a steric barrier that impairs ^{99m}Tc-HMPAO diffusion from NC structure to protein binding sites (Fig. 2D). It is another hypothesis to explain the differences in the release profiles found between the two types of NC studied. The result obtained with conventional PLA nanocapsules showed that approximately 80% of the radioactivity was released in 120 min of incubation. These data are in agreement with the studies of Mosqueira et al. (2006) where a better ability to retain lipophilic antimalarial drug was observed with PLA-PEG NC when compared with PLA NC stabilized with poloxamer in media containing plasma. Poloxamer seems to play an important role in release profiles of lipophilic drugs from NC, because it was able to increase the percentage and the rate of halofantrine release, when it was added to the PLA-PEG NC formulation (Mosqueira et al., 2006).

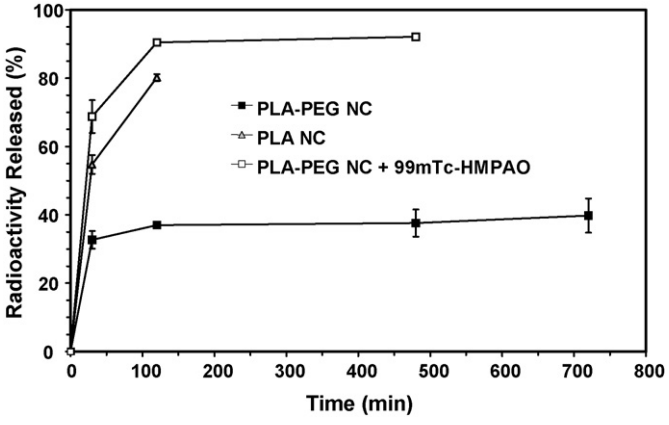

Fig. 6 – Release profiles of ^{99m}Tc-HMPAO encapsulated in PLA(▲) and in PLA-PEG NC (■) and release profile ^{99m}Tc-HMPAO just incubated with preformed PLA-PEG NC (□) in the 70% rat plasma/saline medium at 37 °C (3.4 μg HMPAO/mL of release medium) using 0.1 μm ultrafiltration membrane pore (Millipore®) to separate the nanocapsules from the external medium.

Therefore, the developed PLA-PEG NC emerged as very suitable carrier for transporting ^{99m}Tc-HMPAO radioactive tracer compared to conventional PLA NC preparation to be used in

further pre-clinical experiments for diagnosis of inflammatory processes.

4. Conclusion

Both types of nanocapsules preparations studied in this work were able to encapsulate the ^{99m}Tc-HMPAO with the same yield. However, the physical and structural properties of PLA-PEG nanocapsules to which PEG chains are covalently linked were more homogeneous, as shown by AFM. Indeed, the release profiles of these nanocapsules indicate that a part of the radioactivity was probably adsorbed at the NC surface and presents a burst effect after dilution. However, the greater part of the radioactivity was truly associated with the NC inner structure, and a reduced release rate was observed even in the presence of plasma in the external medium. The better release profile of ^{99m}Tc-HMPAO from PLA-PEG NC, the homogeneity of the polymeric wall and the adequate size indicate that this approach could provide an imaging agent for diagnosis.

Acknowledgments

The authors thank CAPES-Brazil for personal financial support for the first author. This work was supported by the FAPEMIG/NANOBIOMG network. The authors are grateful to Dr. Elenara L. Sena (UFSC-Brazil) for the kind gift of the PLA-PEG polymers purchased from Alkermes. We acknowledge also Dr. Monica C. Oliveira and Danielle N. Assis for their helpful discussions and Dr. David L. Nelson for English revision of the article.

REFERENCES

Assis, D.N., Mosqueira, V.C.F., Vilela, J.M.C., Andrade, M.S., Cardoso, V.N., 2007. Release profiles and morphological characterization by atomic force microscopy and photon correlation spectroscopy of ^{99m}Technetium-fluconazole nanocapsules. Int. J. Pharm., doi:10.1016/j.ijpharm.2007.08.002.

Barratt, G., 2000. Therapeutic applications of colloidal drug carriers. Pharm. Sci. Technol. Today 3, 163–171.

Barthel, H., Kampfer, I., Seese, A., Dannenber, C., Kluge, R., Burchert, W., Knapp, W.H., 1999. Improvement of brain SPECT by stabilization of Tc-99m-HMPAO with methylene blue or cobalt chloride. Nuklearmedizin 38, 80–84.

Boerman, O.C., Laverman, P., Oyen, W.J.G., Corstens, F.H.M., Storm, G., 2000. Radiolabelled liposomes for scintigrafic imaging. Prog. Lipid Res. 39, 461–475.

Brouwers, A.H., De Jong, D.J., Dams, E.T.M., Oyen, W.J.G., Boerman, O.C., Laverman, P., Naber, T.H.J., Storm, G., Corstens, F.H.M., 2000. Tc-99m-PEG-Liposomes for the evaluation of colitis in Crohn's disease. J. Drug Target 8, 225–233.

Chianelli, M., Mather, S.J., Martin-Comin, J., Signore, A., 1997. Radiopharmaceuticals for the study of inflammatory processes: a review. Nucl. Med. Commun. 18, 437–455.

Cruz, L., Soares, L.U., Costa, T.D., Mezzalira, G., Silveira, N.P., Guterres, S.S., Pohlmann, A.R., 2006. Diffusion and mathematical modeling of release profiles from nanocarriers. Int. J. Pharm. 313, 198–205.

Dams, E.T.M., Oyen, W.J.G., Boerman, O.C., Storm, G., Laverman, P., Kok, P.J.M., Buijs, W.C.A.M., Bakker, H., Meer, J.W.M., van der Corstens, F.H.M., 2000. ^{99m}Tc–PEG liposomes for the scintigraphic detection of infection and inflammation: clinical evaluation. J. Nucl. Med. 41, 622–630.

Fessi, H., Puisieux, F., Devissaguet, J.P., Ammoury, N., Benita, S., 1989. Nanocapsule formation by interfacial polymer deposition following solvent displacement. Int. J. Pharm. 55, R1–R4.

Goins, B., Klipper, R., Rudolph, A.S., Cliff, R.O., Blumhardt, R., Phillips, W.T., 1993. Biodistribution and imaging studies of Tc-99m-labelled liposomes in rats. J. Nucl. Med. 34, 2160–2168.

Govender, T., Riley, T., Ehtezazi, T., Garnett, M.C., Stolnik, S., Illum, L., Davis, S., 2000. Defining the drug incorporation properties of PLA-PEG nanoparticles. Int. J. Pharm. 199, 95–110.

Gref, R., Minmitake, Y., Percchia, M.T., Trubetskoy, V., Torchilin, V., Langer, R., 1994. Biodegradable long-circulating polymeric nanospheres. Science 263, 1600–1603.

Laverman, P., Dams, E.T.M., Oyen, W.J.G., Storm, G., Koenders, E.B., Prevost, R., van der Meer, J.W.M., Corstens, F.H.M., Boerman, O.C., 1999. A novel method to label liposomes with ^{99m}Tc by the hydrazino nicotinyl derivate. J. Nucl. Med. 40, 192–197.

Legrand, P., Barratt, G., Mosqueira, V., Fessi, H., Devissaguet, J.P., 1999. Polymeric nanocapsules as drug delivery systems. A review. STP Pharma. Sci. 9, 411–418.

Leite, E.A., Vilela, J.M.C., Mosqueira, V.C.F., Andrade, M.S., 2005. Poly-caprolactone nanocapsules morphological features by atomic force microscopy. Microsc. Microanal. 11, 48–51.

Litzinger, D.C., Buiting, A.M.J., van Rooijen, N., Huang, L., 1994. Effect of liposome size on the circulation time and intraorgan distribution of amphipathic poly(ethylene glycol)-containing liposomes. Biochem. Biophys. Acta Biomembr. 1190, 99–107.

Lopes, E., Pohlmann, A.R., Bassani, V., Guterres, S.S., 2000. Polymeric colloidal systems containing ethionamide: preparation and physico-chemical characterization. Pharmazie 55, 527–530.

Martin-Comin, J., Prats, E., 1999. Clinical applications of radiolabelled blood elements in inflammatory bowel disease. Q. J. Nucl. Med. 43, 74–82.

Mosqueira, V.C.F., Legrand, P., Gref, R., Heurtault, B., Appel, M., Barrat, G., 1999. Interactions between a macrophage cell line (J774A1) and surface-modified poly(D L-lactide) nanocapsules bearing poly(ethylene glycol). J. Drug Target 7, 65–78.

Mosqueira, V.C.F., Legrand, P., Gulik, A., Bourdon, O., Gref, R., Labarre, D., Barratt, G., 2001a. Relationship between complement activation, cellular uptake and physicochemical aspects of novel PEG-modified nanocapsules. Biomaterials 22, 2967–2979.

Mosqueira, V.C.F., Legrand, P., Morgat, J.-P., Vert, M., Mysiakine, E., Gref, R., Devissaguet, J., Barratt, G., 2001b. Biodistribution of long-circulating PEG-grafted nanocapsules in mice: effects of PEG chain length and density. Pharm. Res. 18 (10), 1411–1419.

Mosqueira, V.C.F., Leite, E.A., Barros, C.M., Vilela, J.M.C., Andrade, M.S., 2005. Polymeric nanostructures for drug delivery: characterization by atomic force microscopy. Microsc. Microanal. 11, 36–39.

Mosqueira, V.C.F., Legrand, P., Barratt, G., 2006. Surface-modified and conventional nanocapsules as novel formulation for parenteral delivery of halofantrine. J. Nanosci. Nanotechnol. 9/10, 3193–3202.

Neves, B.R.A., Vilela, J.M.C., Andrade, M.S., 1998. Microscopia de varredura por sonda mecânica: uma introdução. Cerâmica 44, 212–219.

Owens III, D.E., Peppas, N.A., 2006. Opsonization, biodistribution, and pharmacokinetics of polymeric nanoparticles. Int. J. Pharm. 307, 93–102.

Oyen, W.J.G., Boerman, O.C., Storm, G., van Bloois, L., Koenders, E.B., Claessens, R.A.M.J., Perenboom, R.M., Crommelin, D.J.A., van der Meer, J.W.M., Corstens, F.H.M., 1996a. Detecting infection and inflammation with Tc99m-labeled Stealth® liposomes. J. Nucl. Med. 37, 1392–1397.

Oyen, W.J.G., Boerman, O.C., van der Laken, C.J., Claessens, R.A.M.J., van der Meer, J.W.M., Corstens, F.H.M., 1996b. The uptake mechanisms of inflammation and infection-localizing agents. Eur. J. Nucl. Med. 23, 459–465.

Phillips, W.T., 1998. Targeting of drugs 6: strategies for stealth therapeutic systems. In: Gregoriadis, McCormack (Eds.), Use of Radiolabelled Liposomes for PEG-Liposome-based Drug Targeting and Diagnostic Imaging Applications. Plenum Press, New York, pp. 109–120.

Rennen, H.J.J.M., Boerman, O.C., Oyen, W.J.G., Corstens, F.H.M., 2001. Imaging infection/inflammation in the new miliennium. Eur. J. Nucl. Med. 28, 241–252.

Rübe, A., Hause, G., Mäder, K., Kohlbrecher, J., 2005. Core-shell structure of miglyol/poly(D L-lactide)/poloxamer nanocapsules studied by small-angle neutron scattering. J. Control. Release 107, 244–252.

Ruozi, B., Tosi, G., Forni, F., Fresta, M., Vandelli, M.A., 2005. Atomic force microscopy and photon correlation spectroscopy: two techniques for rapid characterization of liposomes. Eur. J. Pharm. Sci. 25, 81–89.

Sasatsu, M., Onishi, H., Machida, Y., 2006. In vitro and in vivo characterization of nanoparticles made of MeO–PEG amine/PLA block copolymer and PLA. Int. J. Pharm. 317, 167–174.

Sobal, G., Sinzinger, H., 2001. Methylene blue-enhanced stability of (^{99m}Tc)HMPAO and simplified quality control—a comparative investigation. Appl. Radiat. Isot. 54, 633–636.

Soppimath, K.S., Aminabhavi, T.M., Kulkarni, A.R., Rudzinski, W.E., 2001. Biodegradable polymeric nanoparticles as drug delivery devices. J. Control Release 70, 1–20.

Szebeni, J., Baranyi, L., Savay, S., Bodo, M., Morse, D.S., Basta, M., Stahl, G.L., Bunger, R., Alving, C.R., 2000. Liposome-induced pulmonary hipertension: properties and mechanism of a complement-mediated pseudoallergic reaction. Am. J. Physiol. Heart Circ. Physiol. 279, H1319–H1328.

Szebeni, J., Baranyi, L., Savay, S., Milosevits, J., Bunger, R., Laverman, P., Metselaar, J.M., Storm, G., Chanan-Khan, A., Liebes, L., Muggia, F.M., Cohen, R., Barenholz, Y., Alving, C.R., 2002. Role of complement activation in hipersensitivity reactions to Doxil and Hynic PEG liposomes: experimental and clinical studies. J. Liposome Res. 12, 165–172.

Vanderghinste, D., Van Eeckhoudt, M., Terwinghe, C., Mortelmans, L., Bormans, G.M., Verbruggen, A.M., Vanbilloen, H.P., 2003. An efficient HPLC method for the analysis of isomeric purity of technetium-99m-exametazime and identity confirmation using LC–MS. J. Pharm. Biom. Anal. 32, 679–685.